ential impairment of GABAergic functions rather than that of pyramidal neurons was consistent with our previous findings that the changes in channel properties with the N1417H mutation were observed only in hippocampal bipolar interneurons, but not in pyramidal neurons [1], which was probably due to specific expression of $Na_v1.1$ channels in GABAergic neurons [9,20].

The present study demonstrated for the first time that the *Scn1a* missense mutation impairs $GABA_A$ receptor-mediated synaptic transmission in the hippocampus. The disruption of GABAergic neurotransmission in Hiss rats can account for their vulnerability to PTZ-induced seizures [1]. More importantly, since hyperthermia per se is known to suppress the GABAergic neurotransmissions in the hippocampus [26–30], the impairment of GABAergic functions by the *Scn1a* mutation seems to be directly linked to the vulnerability to hyperthermic seizures.

The N1417H mutation in Hiss rats caused loss-of-function changes in the $Na_v1.1$ channel properties, a hyperpolarized shift in the voltage-dependency of the channel inactivation and a reduced amplitude of the evoked spikes in GABAergic neurons [1]. However, since the N1417H mutation did not cause a significant reduction in the $Na_v1.1$ sodium currents, these changes in $Na_v1.1$ channel properties were considered to be milder as compared to those reported for the truncated mutations [9,20]. Even though, Hiss rats were distinct from the control animals, exhibiting a significant inhibition in GABAergic neurotransmission as well as a high susceptibility to FS or PTZ seizures. Our results support the notion [8] that even mild loss-of-function mutations in $Na_v1.1$ channels can cause a significant vulnerability to FS by disrupting the GABAergic neurotransmissions. This may be due to the following possibilities. (1) N1417H mutation inhibited the GABAergic activity by reducing axonal excitability (i.e., propagation of action potentials), since recent analysis revealed that *Scn1a* are expressed not only in the somata of GABAergic neurons, but also in their proximal and distal axons [20]. (2) *In vivo* influences of *Scn1a* mutations may turn out to be more intense by the multiple and convergent projections of GABAergic neurons onto the pyramidal neurons, leading to synchronized or magnified influences of GABAergic impairment. Finally, as described previously, (3) hyperthermic stimuli per se inhibit hippocampal GABAergic neurotransmission [26–30].

In conclusion, the present study demonstrated that the N1417H missense mutation in Hiss rats preferentially impairs $GABA_A$ receptor-mediated inhibitory synaptic transmission without significantly altering the excitability of the pyramidal neurons in the hippocampus. Since hyperthermia per se is known to inhibit GABAergic neurotransmission [26–30], the present results strongly suggest that the missense mutations of *Scn1a* gene play a crucial role in the pathogenesis of human FS by disrupting the hippocampal GABAergic neurotransmission.

## Acknowledgments

This study was supported in part by a research grant from the Japan Epilepsy Research Foundation; a Grant-in-Aid for Scientific Research from the Ministry of Education, Culture, Sports, Science and Technology of Japan (Nos. 20240042 and 22590092). We are also thankful to the National BioResource Project-Rat for providing Hiss rat (#0455) (http://www.anim.med.kyoto-u.ac.jp/NBR/).

## References

[1] T. Mashimo, I. Ohmori, M. Ouchida, Y. Ohno, T. Tsurumi, T. Miki, M. Wakamori, S. Ishihara, T. Yoshida, A. Takizawa, M. Kato, M. Hirabayashi, M. Sasa, Y. Mori, T. Serikawa, A missense mutation of the gene encoding voltage-dependent sodium channel ($Na_v1.1$) confers susceptibility to febrile seizures in rats, J. Neurosci. 30 (2010) 5744–5753.
[2] S. Shinnar, Febrile seizures and mesial temporal sclerosis, Epilepsy Cur. 3 (2003) 115–118.
[3] S. Baulac, I. Gourfinkel-An, R. Nabbout, G. Huberfeld, J. Serratosa, E. Leguern, M. Baulac, Fever genes and epilepsy, Lancet Neurol. 3 (2004) 421–430.
[4] A. Fetveit, Assessment of febrile seizures in children, Eur. J. Pediatr. 167 (2008) 17–27.
[5] M.H. Scantlebury, J.G. Heida, Febrile seizures and temporal lobe epileptogenesis, Epilepsy Res. 89 (2010) 27–33.
[6] M.H. Meisler, J.A. Kearney, Sodium channel mutations in epilepsy and other neurological disorders, J. Clin. Invest. 115 (2005) 2010–2017.
[7] D.S. Ragsdale, How do mutant $Na_v1.1$ sodium channels cause epilepsy?, Brain Res Rev. 58 (2008) 149–159.
[8] W.A. Catterall, F. Kalume, J.C. Oakley, $Na_v1.1$ channels and epilepsy, J. Physiol. 588 (Pt11) (2010) 1849–1859.
[9] F.H. Yu, M. Mantegazza, R.E. Westenbroek, C.A. Robbins, F. Kalume, K.A. Burton, W.J. Spain, G.S. McKnight, T. Scheuer, W.A. Catterall, Reduced sodium current in GABAergic interneurons in a mouse model of severe myoclonic epilepsy in infancy, Nat. Neurosci. 9 (2006) 1142–1149.
[10] J.C. Oakley, F. Kalume, F.H. Yu, T. Scheuer, W.A. Catterall, Temperature- and age-dependent seizures in a mouse model of severe myoclonic epilepsy in infancy, Proc. Natl. Acad. Sci. USA 106 (2009) 3994–3999.
[11] M.S. Martin, K. Dutt, L.A. Papale, C.M. Dube, S.B. Dutton, G. de Haan, A. Shankar, S. Tufik, M.H. Meisler, T.Z. Baram, A.L. Goldin, A. Escayg, Altered function of the SCN1A voltage-gated sodium channel leads to gamma-aminobutyric acid-ergic (GABAergic) interneuron abnormalities, J. Biol. Chem. 285 (2010) 9823–9834.
[12] A. Akaike, Y. Ohno, M. Sasa, S. Takaori, Excitatory and inhibitory effects of dopamine on neuronal activity of the caudate nucleus neurons in vitro, Brain Res. 418 (1987) 262–272.
[13] Y. Ohno, J.E. Warnick, Effects of thyrotropin-releasing hormone on phencyclidine- and ketamine-induced spinal depression in neonatal rats, Neuropharmacology 27 (1988) 1013–1018.
[14] Y. Ohno, J.E. Warnick, Selective depression of the segmental polysynaptic reflex by phencyclidine and its analogs in the rat in vitro: interaction with *N*-Methyl-D-Aspartate receptors, J. Pharmacol. Exp. Ther. 252 (1990) 246–252.
[15] G. Paxinos, C. Watson, The Rat Brain in Stereotaxic Coordinates, 6th ed., Elsevier, Massachussets, 2007.
[16] R. Lipowsky, R. Gillessen, C. Alzheimer, Dendritic $Na^+$ channels amplify EPSPs in hippocampal CA1 pyramidal cells, J. Neurophysiol. 76 (1996) 2181–2191.
[17] Y. Ohno, S. Ishihara, R. Terada, M. Kikuta, N. Sofue, Y. Kawai, T. Serikawa, M. Sasa, Preferential increase in the hippocampal synaptic vesicle protein 2A (SV2A) by pentylenetetrazole kindling, Biochem. Biophys. Res. Commun. 390 (2009) 415–420.
[18] N. Collinson, F.M. Kuenzi, W. Jarolimek, K.A. Maubach, R. Cothliff, C. Sur, A. Smith, F.M. Otu, O. Howell, J.R. Atack, R.M. McKernan, G.R. Seabrook, G.R. Dawson, P.J. Whiting, T.W. Rosahl, Enhanced learning and memory and altered GABAergic synaptic transmission in mice lacking the alpha 5 subunit of the $GABA_A$ receptor, J. Neurosci. 22 (2002) 5572–5580.
[19] W.R. Proctor, L. Diao, R.K. Freund, M.D. Browning, P.H. Wu, Synaptic GABAergic and glutamatergic mechanisms underlying alcohol sensitivity in mouse hippocampal neurons, J. Physiol. 575 (2006) 145–159.
[20] I. Ogiwara, H. Miyamoto, N. Morita, N. Atapour, E. Mazaki, I. Inoue, T. Takeuchi, S. Itohara, Y. Yanagawa, K. Obata, T. Furuichi, T.K. Hensch, K. Yamakawa, $Na_v1.1$ localizes to axons of parvalbumin-positive inhibitory interneurons: a circuit basis for epileptic seizures in mice carrying an *Scn1a* gene mutation, J. Neurosci. 27 (2007) 5903–5914.
[21] C. Lossin, D.W. Wang, T.H. Rhodes, C.G. Vanoye, A.L. George Jr., Molecular basis of an inherited epilepsy, Neuron 34 (2002) 877–884.
[22] P. Cossette, A. Loukas, R.G. Lafrenière, D. Rochefort, E. Harvey-Girard, D.S. Ragsdale, R.J. Dunn, G.A. Rouleau, Functional characterization of the D188V mutation in neuronal voltage-gated sodium channel causing generalized epilepsy with febrile seizures plus (GEFS), Epilepsy Res. 53 (2003) 107–117.
[23] C. Lossin, T.H. Rhodes, R.R. Desai, C.G. Vanoye, D. Wang, S. Carniciu, O. Devinsky, A.L. George Jr., Epilepsy-associated dysfunction in the voltage-gated neuronal sodium channel SCN1A, J. Neurosci. 23 (2003) 11289–11295.
[24] T.H. Rhodes, C. Lossin, C.G. Vanoye, D.W. Wang, A.L. George Jr., Noninactivating voltage-gated sodium channels in severe myoclonic epilepsy of infancy, Proc. Natl. Acad. Sci. USA 101 (2004) 11147–11152.
[25] J. Spampanato, J.A. Kearney, G. de Haan, D.P. McEwen, A. Escayg, I. Aradi, B.T. MacDonald, S.I. Levin, I. Soltesz, P. Benna, E. Montalenti, L.L. Isom, A.L. Goldin, M.H. Meisler, A novel epilepsy mutation in the sodium channel SCN1A identifies a cytoplasmic domain for beta subunit interaction, J. Neurosci. 24 (2004) 10022–10034.
[26] J. Wu, S.P. Javedan, K. Ellsworth, K. Smith, R.S. Fisher, Gamma oscillation underlies hyperthermia-induced epileptiform-like spikes in immature rat hippocampal slices, BMC Neurosci. 2 (2001) 18.
[27] J.Q. Kang, W. Shen, R.L. Macdonald, Why does fever trigger febrile seizures? $GABA_A$ receptor gamma2 subunit mutations associated with idiopathic generalized epilepsies have temperature-dependent trafficking deficiencies, J. Neurosci. 26 (2006) 2590–2597.
[28] L. Qu, X. Liu, C. Wu, L.S. Leung, Hyperthermia decreases GABAergic synaptic transmission in hippocampal neurons of immature rats, Neurobiol. Dis. 27 (2007) 320–327.
[29] L. Qu, L.S. Leung, Mechanisms of hyperthermia-induced depression of GABAergic synaptic transmission in the immature rat hippocampus, J. Neurochem. 106 (2008) 2158–2169.
[30] L. Qu, L.S. Leung, Effects of temperature elevation on neuronal inhibition in hippocampal neurons of immature and mature rats, J. Neurosci. Res. 87 (2009) 2773–2785.

*Exp. Anim. 59(4), 531–535, 2010*

—Note—

# Survey of Live Laboratory Animals Reared in Japan (2009)

Ken-ichi YAGAMI, Tomoji MASHIMO, Fujio SEKIGUCHI, Fumihiro SUGIYAMA, Ken-ichi YAMAMURA, and Tadao SERIKAWA

*JALAS Board of Executive Directors, Japanese Association for Laboratory Animal Science, Akamon Royal Heights, Rm 1103, 5–29–12 Hongo, Bunkyo-ku, Tokyo 113-0033, Japan*

**Abstract:** A survey on the number of live laboratory animals reared in research institutions, including universities, biomedical institutes, testing laboratories, pharmaceutical companies, and animal breeders, was conducted on June 1, 2009. One thousand seventy-four replies were recovered from 1,593 institutions, and 471 of them had used live laboratory animals from June 1, 2008 to May 31, 2009. A total of 11,337,334 live laboratory animals were being maintained on June 1, 2009 in Japan.

**Key words:** Japan, laboratory animals, survey

In Japan, animal experiments are regulated by the "Law for the Humane Treatment and Management of Animals" [7] and the "Standards Relating to the Care and Management of Laboratory Animals and Relief of Pain" [8]. Furthermore, the Fundamental Guidelines for Proper Conduct of Animal Experiment were established by the Japanese Government (Ministry of Education, Culture, Sports, Science and Technology, Ministry of Health, Labour and Welfare, and Ministry of Agriculture, Forestry and Fisheries) [6], and the "Guidelines for Proper Conduct of Animal Experiments" was also provided by the Science Council of Japan [9], on June 1, 2006. Thus, a dual system for animal experiments with regulations and guidelines has been reconstructed in Japan and strengthened to reach a social consensus on the necessity of animal experiments with a minimum regulatory restriction on science and technology [5]. The Japanese Association for Laboratory Animal Science (JALAS) has carried out surveys concerning the use of live laboratory animals and reported regularly [1–4]. In the latest survey, we improved questionnaires by making them simpler and objective-oriented to elucidate the situation of animal experiments nation-wide.

The questionnaires were distributed to a total of 1,593 institutions including whole universities, colleges and junior colleges (1,287), government institutes, incorporated administrative agencies and public interest corporations (172), and companies which are corporate members of JALAS (134). For a comprehensive survey, we asked the Japan Pharmaceutical Manufacturers Association (JPMA), the Japanese Society for Laboratory Animal Resources (JSLA), the Japan Association of Contract Laboratories for Safety Evaluation (JACL), and the Japan Cooperative Association for Laboratory Animals (JCALA) for their support.

Out of 1,593 distributed questionnaires, replies were received from 1,074 (67.4%) institutions. Four hundreds seventy-one institutions of them had used live labora-

*(Received 12 April 2010 / Accepted 28 April 2010)*

*Address corresponding: K. Yagami, Laboratory Animal Resource Center, University of Tsukuba, 1–1–1 Tennodai, Tsukuba, Ibaraki 305-8575, Japan*

**Table 1.** Number of institutions using live laboratory animals in Japan

| Institutions | No. of questionnaires addressed | No. of replies | Reply ratio (%) | Use of laboratory animals* | |
|---|---|---|---|---|---|
| | | | | Yes | No |
| Universities | 1,287 | 862 | 67.0 | 326 | 536 |
| Institutes | 172 | 127 | 73.8 | 89 | 38 |
| Companies | 134 | 85 | 63.4 | 56 | 29 |
| Total | 1,593 | 1,074 | 67.4 | 471 | 603 |

*Use of laboratory animals for the past year from June 1, 2008 to May 31, 2009.

**Table 2.** Numbers of live laboratory animals being maintained in Japan (On June 1, 2009)

| Categories | Species | Universities | Institutes | Companies | Total |
|---|---|---|---|---|---|
| Mammal | Mice | 6,729,403 | 407,579 | 2,396,799 | 9,533,781 |
| | (GM-mice)* | (3,248,993) | (197,455) | (119,392) | (3,565,840) |
| | Rats | 570,015 | 19,478 | 774,119 | 1,363,612 |
| | (GM-rats)* | (7,000) | (524) | (5,742) | (13,266) |
| | Hamsters | 29,737 | 277 | 18,988 | 49,002 |
| | Guinea pigs | 6,455 | 365 | 191,255 | 198,075 |
| | Laboratory shrew | 803 | 515 | 30 | 1,348 |
| | Rabbits | 36,115 | 416 | 13,699 | 50,230 |
| | Dogs | 3,473 | 1,152 | 4,370 | 8,995 |
| | Cats | 670 | 237 | 191 | 1,098 |
| | Ferrets | 59 | 3 | 239 | 301 |
| | Pigs | 578 | 901 | 28 | 1,507 |
| | Goats | 179 | 74 | 63 | 316 |
| | Sheep | 404 | 134 | 0 | 538 |
| | Cattle | 828 | 313 | 49 | 1,190 |
| | Horse | 47 | 43 | 0 | 90 |
| | Macaque monkeys | 1,702 | 2,193 | 6,021 | 9,916 |
| | Squirrel monkeys | 48 | 11 | 0 | 59 |
| | Marmosets | 156 | 819 | 302 | 1,277 |
| | Other rodents | 81,355 | 618 | 18 | 81,991 |
| | Other carnivora | 65 | 18 | 0 | 83 |
| | Other artiodactyla | 2 | 0 | 0 | 2 |
| | Other primates | 36 | 115 | 23 | 174 |
| | Other mammals | 378 | 0 | 0 | 378 |
| | Sub-total | 7,462,508 | 435,261 | 3,406,194 | 11,303,963 |
| Birds | Chickens | 7,765 | 6,575 | 11,401 | 25,741 |
| | Japanese quails | 2,259 | 1,465 | 0 | 3,724 |
| | Geese | 0 | 14 | 0 | 14 |
| | Pigeons | 325 | 0 | 0 | 325 |
| | Other birds | 1,013 | 1,242 | 0 | 2,255 |
| | Sub-total | 11,362 | 9,296 | 11,401 | 32,059 |
| Reptiles | Snakes | 33 | 1,007 | 0 | 1,040 |
| | Turtles | 95 | 0 | 0 | 95 |
| | Lizards | 123 | 0 | 0 | 123 |
| | Other reptiles | 54 | 0 | 0 | 54 |
| | Sub-total | 305 | 1,007 | 0 | 1,312 |
| Total | | 7,474,175 | 445,564 | 3,417,595 | 11,337,334 |

* Numbers of GM-mice (genetically modified mice) or GM-rats (genetically modified rats) are shown in parenthesis, and included in numbers of mice or rats.

tory animals in the past year from June 1, 2008 to May 31, 2009, meaning that a total of 471 institutions (universities and colleges, 326; institutes, 89; companies, 56) performed animal experiments during that period in Japan (Table 1).

Species and numbers of reared laboratory animals on June 1, 2009 are shown in Table 2. Of 11,337,334 live laboratory animals reared in Japan, 9,533,781 (84.1%) of them were mice, and 1,363,612 (12.0%) were rats. Approximately 99% of live laboratory animals were rodents including mice and rats. Genetically modified mice represented 37.4% of the number of mice reared, and genetically modified rats were 0.97% of the total number of rats. As major laboratory animals other than rodents, 50,230 (0.4%) rabbits and 11,426 (0.1%) primates such as macaque, squirrel monkeys, and marmosets were reared.

These data are one of important information about the current situation of animal experiments in Japan, though there were minor differences in questionnaire items and objectives compared to the previously reported surveys. We will continue to conduct surveys regularly, and provide more accurate information concerning animal experiments in Japan to foster social understanding for animal experiments.

## References


1. JALAS Committee for Laboratory Animal Care and Use. 2003. *Jikken Doubutsu News* 52: 143 (in Japanese).
2. JALAS Committee for Laboratory Animal Care and Use. 2007. *Jikken Doubutsu News* 56: 11 (in Japanese).
3. JALAS Working Group for Laboratory Animal Data Bank. 1998. *Jikken Doubutsu News* 47: 58 (in Japanese).
4. JALAS Working Group for Laboratory Animal Data Bank. 2001. *Jikken Doubutsu News* 50: 57 (in Japanese).
5. Kagiyama, N., Ikeda, T., and Nomura, T. 2006. pp. 187–191. *In*: In vivo Models of Inflammation Vol. 1 (Stevenson, S.C., Marshall, L.A., and Morgan, D.W. eds.), Birkhaeuser Verlag, Basel.
6. Ministry of Education, Culture, Sport, Science and Technology. 2006. Fundamental Guidelines for Proper Conduct of Animal Experiment and Related Activities in Academic Research Institutions. [Online] http://www.mext.go.jp/b_menu/hakusho/nc/06060904.htm (in Japanese).
7. Ministry of the Environment. 2005. The Law for the Humane Treatment and Management of Animals. [Online] http://law.e-gov.go.jp/htmldata/S48/S48HO105.html (in Japanese).
8. Ministry of the Environment. 2006. The Standards Relating to the Care and Management of Laboratory Animals and Relief of Pain. [Online] http://www.env.go.jp/nature/dobutsu/aigo/2_data/nt_h180428_88.html (in Japanese).
9. Science Council of Japan. 2006. Guidelines for Proper Conduct of Animal Experiments. [Online] http://www.scj.go.jp/ja/info/kohyo/2006.html

## <Appendix>

### Questionnaire for Use of Live Laboratory Animals

About your institutions

| | |
|---|---|
| Name of Institutions | |
| Address | |
| TEL and FAX | |
| Position of Respondent | |
| Name of Respondent | |
| Category of Institutions* | ☐ University ☐ Institute ☐ Company ☐ Other ( ) |

* Check applicable square.

1) At your institution, did you use live laboratory animals for education, research, testing, manufacture of biological products, or other scientific purposes in the past year from June 1, 2008 to May 31, 2009?
Check applicable square.

☐ Yes ☐ No

2) Fill in the numbers of live laboratory animals being maintained at your institution on June 1, 2009 in the following Table.

| Categories | Species | Numbers of Reared Live Animals |
|---|---|---|
| Mammal | Mice | |
| | (GM-mice)* | |
| | Rats | |
| | (GM-rats)* | |
| | Hamsters | |
| | Guinea pigs | |
| | Laboratory shrew | |
| | Rabbits | |
| | Dogs | |
| | Cats | |
| | Ferrets | |
| | Pigs | |
| | Goats | |
| | Sheep | |
| | Cattle | |
| | Horse | |
| | Macaque monkeys | |
| | Squirrel monkeys | |
| | Marmosets | |
| | Other rodents | |
| | Other carnivora | |
| | Other artiodactyla | |
| | Other primates | |
| | Other mammals | |
| Birds | Chickens | |
| | Japanese quails | |
| | Geese | |
| | Pigeons | |
| | Other birds | |
| Reptiles | Snakes | |
| | Turtles | |
| | Lizards | |
| | Other reptiles | |

* Please show numbers of GM-mice (genetically modified mice) or GM-rats (genetically modified rats) were shown in parenthesis, and included in numbers of mice or rats.

Notes

1) Principally, live animals mean individuals after weaning.
2) Approximate numbers may be calculated from cage numbers in for animals which are generally maintained with cage mates such as rodents.
3) Genetically modified mice (rats) means transgenic mice (rats), knockout mice, knockin mice, and their offsprings, but not mice (rats) injected with recombinant virus vector or recombinant cells.
4) Please contact the JALAS office by a FAX or e-mail, if you have any questions.

Experimental Eye Research 91 (2010) 26–33

Contents lists available at ScienceDirect

Experimental Eye Research

journal homepage: www.elsevier.com/locate/yexer

# A novel middle-wavelength opsin (M-opsin) null-mutation in the retinal cone dysfunction rat

Bei Xie [a,b], Satoshi Nakanishi [b], Qun Guo [a], Feng Xia [a], Guolin Yan [a], Jing An [a], Li Li [a], Tadao Serikawa [b], Takashi Kuramoto [b,**], Zuoming Zhang [a,*]

[a] Department of Clinical Aerospace Medicine, Faculty of Aerospace Medicine, Key Laboratory of Aerospace Medicine of National Education Ministry, Fourth Military Medical University, 17 Changle West Road, Xi'an 710032, China

[b] Institute of Laboratory Animals, Graduate School of Medicine, Kyoto University, Yoshidakonoe-cho, Sakyo-ku, Kyoto 6068501, Japan

ARTICLE INFO

*Article history:*
Received 28 October 2009
Accepted in revised form 29 March 2010
Available online 3 April 2010

*Keywords:*
M-opsin cone dysfunction
deuteranopia
opsin 1, medium-wave sensitive
electroretinogram

ABSTRACT

The disease-causing gene which underlies a naturally occurring X-linked mutant cone dysfunction Sprague–Dawley rat model was investigated. Full-field electroretinogram (ERG) and simple sequence length polymorphism analyses were applied to 441-second filial generation rats that were derived from crossing a mutant rat and a Brown–Norway rat. After identifying a mutation mapping within the telomeric region of chromosome X, a candidate gene related to retinal cone function in this region was further screened using real-time PCR, immunohistochemistry and histological methods. The results showed that a G-to-T substitution at the splice acceptor site of intron 4 was present in the opsin 1, medium-wave sensitive (*Opn1mw*) gene, thereby causing down-regulated transcription and translation. These changes were consistent with abnormities seen in the ERG response. However, there was no significant histological change in the mutant rat retina. Therefore, we infer from this that the causative gene for the mutation is *Opn1mw* and consequently term this a middle-wavelength opsin cone dysfunction (MCD) rat model. The deficiency in vision of the MCD rat is similar to the color vision defects that occur in humans with a color vision defect but without recessive retinal degeneration. This rat model may be useful for understanding the mechanism that is responsible for color vision and for developing clinical therapies for several retinal dystrophies caused by cone opsin deficiencies.



## 1. Introduction

Three types of cones comprise the human retina and are responsible for sensitivity to red, green and blue light, respectively. The degree of sensitivity is dependent on the visual pigment that is contained within the cone. A visual pigment consists of opsin, an apoprotein, which is covalently linked to a small conjugated chromophore, 11-*cis*-retinal or in some cases 11-*cis*-dehydroretinal. Photon absorption by the visual pigments results in visual excitation by causing the chromophore to undergo 11-*cis*- to *trans*-isomerization. Variations in the absorption spectra of different pigments are thought to arise from differences in the primary structure of the apoprotein. Specifically, the visual pigments that mediate color vision are believed to differ in their absorption spectra owing to the attachment of 11-*cis*-retinal to three structurally distinct cone opsins. A corollary to this hypothesis is that colorblindness arises from alterations in the genes which encode the cone opsins (Nathans and Hogness, 1984). Mutations in long-wavelength cone opsin (L-opsin) cause protanopia while mutations in middle-wavelength opsin (M-opsin) result in deuteranopia. Most mutations in deuteranopia were first thought to occur through rearrangements of M-opsin that is encoded by the gene opsin 1, medium-wave sensitive (*Opn1mw*) (Ueyama et al., 2002). However, point mutations have been found in cases of deuteranopia (Winderickx et al., 1992a,b; Ueyama et al., 2002). The point mutations include Cys203-to-Arg, Arg330-to-Gln, Asn94-to-Lys and -71A–C transversion.

In the rat, cones only express two types of cone pigments: short- and middle-wavelength cone opsins, which respond to blue and green light, respectively (Deegan and Jacobs, 1993; Szél and Röhlich, 1992; Yasuo et al., 2002). In humans, the genes that encode red and green pigments on chromosome X are in a head-to-tail tandem array in which a single red pigment gene lies 5′ to one or more nearly identical green pigment genes. In contrast, in the rat only one green pigment gene resides on chromosome X.

* Corresponding author. Tel./fax: +86 29 8477 4817.
** Corresponding author. Tel.: +81 75 753 4494; fax: +81 75 753 4409.
*E-mail addresses:* tkuramot@anim.med.kyoto-u.ac.jp (T. Kuramoto), zhangzm@fmmu.edu.cn (Z. Zhang).

0014-4835/$ – see front matter © 2010 Elsevier Ltd. All rights reserved.
doi:10.1016/j.exer.2010.03.017

The retinal cone dysfunction rat is a naturally occurring mutant model of X-linked cone dysfunction (Zhang et al., 2002). In this model the photopic electroretinogram (ERG) is abnormal. However, there are no obvious histopathological changes or changes in physiological parameters (Gu et al., 2003; Xie et al., 2008). Cone dysfunction does not in this case lead to cone photoreceptor degeneration and may therefore differ from other mouse models of cone dystrophy (Chang et al., 2005, 2006). Here, we identify the molecular basis of this cone dysfunction as a point mutation in the middle-wavelength opsin gene and therefore designate this rat model "MCD" an M-opsin cone dysfunction. The MCD rat may also be considered a model for human blue cone monochromacy (BCM) since it has only a functional S-cone opsin gene.

## 2. Methods

### 2.1. Animals used

MCD model rats that were developed by the Fourth Military Medical University (Gu et al., 2003; Xie et al., 2008; Zhang et al., 2002) were maintained under a 12 h light–dark cycle. Brown–Norway (BN) rats were purchased from Vital River Laboratory Animal Technology Company (Beijing, China). Sprague–Dawley (SD) rats were obtained from the Laboratory Animal Research Center of the Fourth Military Medical University. All procedures which involved animals adhered to the ARVO Statement for the Use of Animals in Ophthalmic and Vision Research and were approved by the Animal Care and Use Committee of the Fourth Military Medical University.

### 2.2. ERG recording

Phenotypes of all of the animals were determined by ERG. ERGs were recorded by using procedures as previously described (Gu et al., 2003; Zhang et al., 2004). In brief, after 10 h of adapting to the dark, the rats were intraperitoneally anesthetized. Their pupils were then dilated by using 0.5% tropicamide. ERGs were recorded off of the corneal surface using a silver-chloride electrode loop encased in a layer of 1% methylcellulose. Stainless steel needle electrodes that had been placed in the cheeks served as reference leads and needles that had been placed in the tails acted as ground leads. ERGs were recorded by using a commercial system (RETIport; Roland Consult GmbH, Brandenburg, Germany) with a band pass of 0.5–1000 Hz. Strobe stimulus flashes were delivered in a Ganzfeld. Dark-adapted 0.01–3 cd s $m^{-2}$ intensity flashes were used to record responses. A steady adapting field of 30 cd $m^{-2}$ was presented within the Ganzfeld. After adapting to the light for 10 min, cone responses were elicited by flash stimuli of 0.01, 0.03, 0.1, 0.3, 1, or 3 cd s $m^{-2}$ and 0.5, 10, or 20 Hz that were superimposed against the adapting field. According to the responses and gender, animals could be classified into four groups. Six rats for each group were used for the ERG analysis.

### 2.3. Structural analysis of the retina

Both eyes from mutant rats and age-matched SD rats were examined at intervals from one to 12 months of age. The eyes were enucleated after each rat had been deeply anesthetized and they were then immersed in 4% paraformaldehyde in 0.1 M phosphate buffer (pH 7.2) for 1 h. The anterior portions of the eyes were then removed, and the posterior portions were fixed for an additional 12 h. The eyecups were dehydrated in an alcohol series and then embedded in paraffin. Sections 5 μm thick were cut along the vertical meridian through the optic nerve head and stained with hematoxylin and eosin. For each animal, results that were obtained from three separate sections were averaged.

### 2.4. Genetic mapping

To create a genetic map of the *mcd* locus, we produced 441-second filial generation (F2) animals. Briefly, female homologous mutant ($X^{mcd}X^{mcd}$) rats were crossed with male wild-type BN ($X^{+}Y$) rats. The resulting first filial generation (F1) rats were intercrossed to obtain F2 rats. ERGs for the F2 animals were recorded at eight weeks of age. Using these, the genotypes for their *mcd* loci were determined. Genotyping for 88 simple sequence length polymorphism markers on chromosome X was carried out using the Ampdirect® Plus and FTA® card (Amp-FTA) methods (Nakanishi et al., 2009). Recombination rates were manually calculated and linkage relationships were evaluated using the chi-square test.

### 2.5. Sequencing

To analyze the *Opn1mw* sequence, we amplified the 6 exons of the gene from the genomic DNA of homozygous MCD ($X^{mcd}X^{mcd}$) and SD ($X^{+}X^{+}$) rats. The primers that were used to amplify exons are listed in Table 1. DNA sequencing was performed as previously described (Kuramoto et al., 2004).

### 2.6. Quantitative real-time PCR

Total RNA was isolated from the retinas using ISOGEN (Nippon gene, Tokyo, Japan) according to the manufacturer's instructions. cDNA was synthesized from 5 μg of total RNA using Super Script III reverse transcriptase (Invitrogen Corp., Carlsbad, CA, USA) and oligo(dT)12–18 primer (Invitrogen Corp., Carlsbad, CA, USA). Real-time PCR was performed using a Thermal Cycler Dice® Real Time System (Takara Bio. Inc., Otsu, Japan) with SYBR Premix Ex Taq II (Takara Bio. Inc., Otsu, Japan). The nucleotide sequences of the PCR primers that were used to quantify the *Opn1mw* transcripts flanked the mutation site and were 5′-catcgtgctctgctacctccaa-3′ and 5′-cagaggcagtatgcgaagacca-3′. The forward primer was located in exon 4 and the reverse primer was in exon 5. By monitoring the amplification curves of a test sample and reference samples that contained $10^{1}$–$10^{6}$ molecules of the gene of interest, the number of target molecules in the test sample could be analyzed. The numbers of target molecules were normalized against that for glyceraldehyde-3-phosphate dehydrogenase (GAPDH) which was used as an endogenous control.

### 2.7. Immunohistochemistry

After anesthetization, eyes were isolated and fixed with 4% paraformaldehyde in 0.1 M phosphate buffer for 12 h. Tissues were cryoprotected by immersion in 20 and 25% sucrose solutions at 4 °C for 24 h in turn. Sections 10 μm thick were rinsed in phosphate buffered saline and blocked with blocking solution consisting of 0.5% Triton X-100 and 10% normal goat serum for

**Table 1**
Primers used for amplifying rat *Opn1mw* exons.

| Primer name | Forward (5′ > 3′) | Reverse (5′ > 3′) |
|---|---|---|
| *Opn1mw.1* | cctgggcccaattaagagat | aacaaacccctctggcatcag |
| *Opn1mw.2* | cccaccccaattgatttatg | ctccaacccttgtgctgact |
| *Opn1mw.3* | catggaagcaaagcagatga | tgtaagcaaggagccacaca |
| *Opn1mw.4* | ggttggggaggttacaggtt | tcaggccagtcacaactgag |
| *Opn1mw.5* | gctcccaagtcaggtcattc | tgcaaggataccagaggtca |
| *Opn1mw.6* | tgagccttcttcatcccact | atctgcaaacatggggactg |

1 h. Slides were incubated with primary antibody (Abcam, Cambridge, MA, USA) at a dilution of 1:2400 overnight at 4 °C and fluorescein-conjugated goat anti-rabbit secondary antibody (ZSGB, Beijing, China) at a dilution of 1:250 for 1 h at room temperature. Retinas were incubated in rhodamine peanut agglutinin (PNA from Vector) at a dilution of 1:200 for 2 h to label the total cone populations. Nuclei were stained with 4′, 6-diamidino-2-phenylindole. The sections were viewed using a laser scanning confocal microscope.

### 2.8. Wholemount immunocytochemistry

Wholemount immunocytochemistry were performed using procedures as previously described (Gu et al., 2003). Eyes were enucleated after an anesthetic overdose and fixed in 4% paraformaldehyde for 1 h. The anterior parts of eyes were then removed, and the eyecups were fixed overnight. The neural retinas were separated from the pigment epithelium, and thoroughly washed. Nonspecific binding was blocked by normal goat serum at room temperature for 1 h. Then the tissues were incubated with primary antibody overnight at 4 °C and FITC-labeled secondary antibody for 1 h at room temperature. After 2 h of incubation with the rhodamine-labeled PNA, the retinas were washed three times and coverslipped. Nuclei were stained with 4′, 6-diamidino-2-phenylindole. All reagents and washing buffers contained 0.1% Triton X-100 to permeabilize membranes. The number of PNA-labeled cells was counted at a location centered 1 mm from the optic nerve head. For each animal, results obtained from five separate sections were averaged.

## 3. Results

### 3.1. ERG responses

All F1 female rats were wild-type heterozygous ($X^{mcd}X^{+}$) and their ERG responses were normal while the F1 male rats were all mutants ($X^{mcd}Y$) and showed abnormal ERG responses (Gu et al., 2003; Zhang et al., 2002). Among 224 F2 females, 104 were mutant homozygotes ($X^{mcd}X^{mcd}$) with abnormal ERG responses and 120 were wild-type heterozygous ($X^{mcd}X^{+}$) with normal ERG responses. Among 217 F2 males, 118 were mutants ($X^{mcd}Y$) and exhibited abnormal ERG responses and 99 were wild-type ($X^{+}Y$) and showed normal ERG responses. The ERG results showed that the inherited trait of the MCD rat strain was recessive. For four genotypes of the F2 rats, the amplitudes of scotopic ERG b-waves that were recorded with serial intensities for the mutant rats were lower than those for wild-type rats. However, there was no significant difference in this experiment as seen in Fig. 1. The amplitudes recorded in heterozygous wild-type female rats were lower than those recorded in wild-type male rats. The differences also made no sense. Photopic cone responses could not be recorded for the MCD rats as previously reported (Gu et al., 2003; Zhang et al., 2002), but they were easily recorded for the wild-type rats. Similar results were found for the flicker ERG responses with serial light intensities and different stimulating frequencies as shown in Fig. 2. The amplitudes that were recorded for the wild-type male rats were significantly higher than those for the wild-type heterozygous female rats. These cumulative results suggested that the mutation causes a severe defect in retinal cone function.

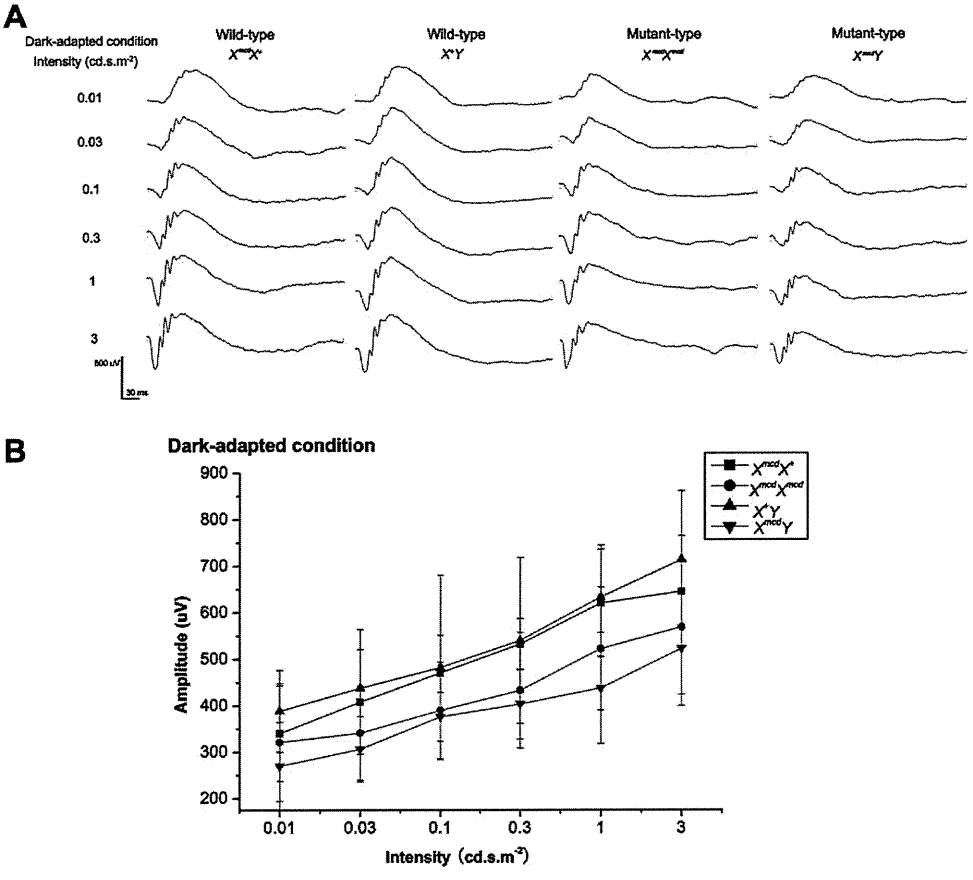


**Fig. 1.** Dark-adapted responses for serial intensity flashes. Six rats for each group were used for the ERG analysis. A: The responses for the dark-adapted condition were detected for all intensities. B: The amplitudes of wild-type rats for dark-adaption were higher than those for the mutant-type rats. The differences were not significant.

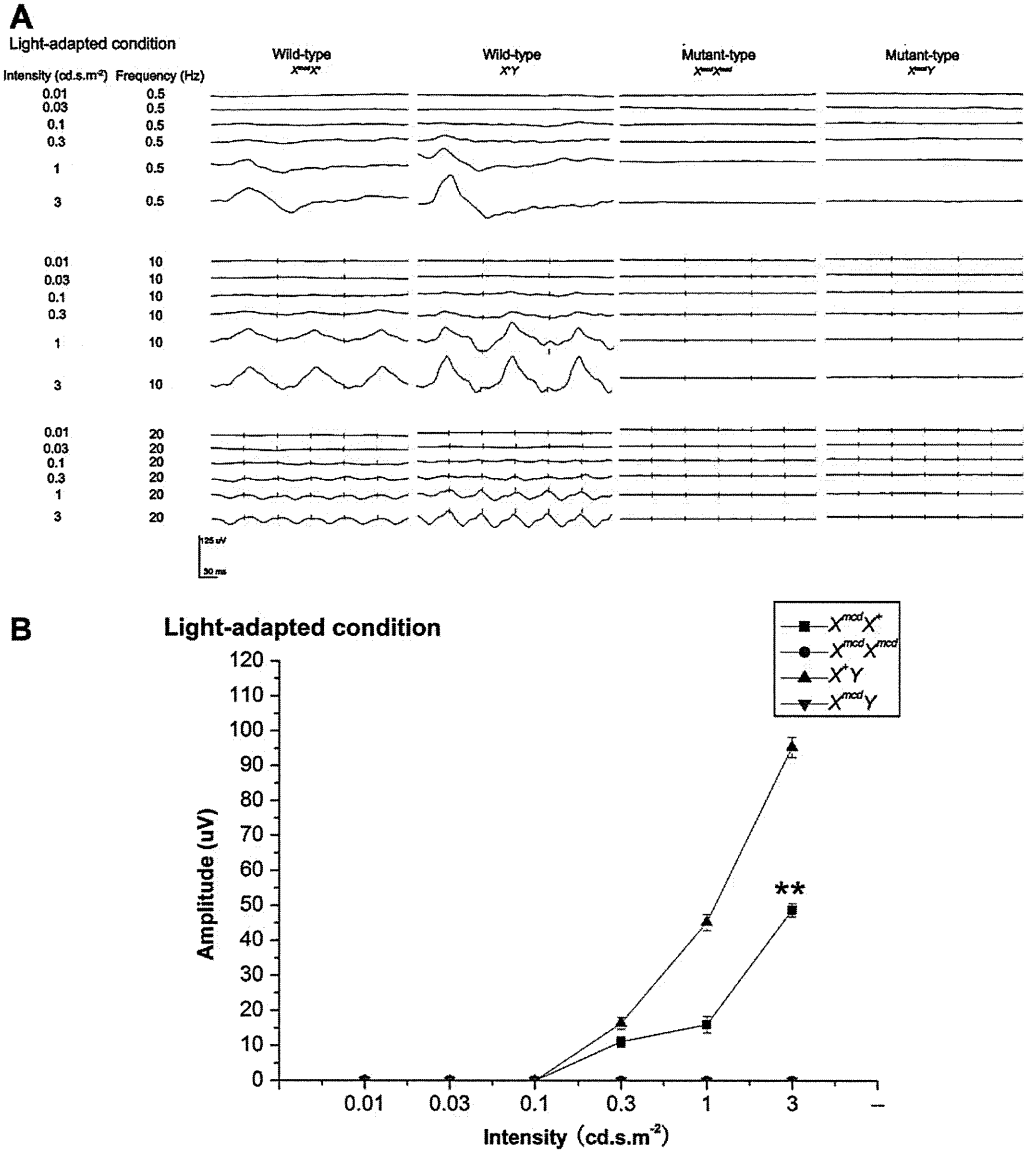


**Fig. 2.** Cone responses for different intensities and frequencies superimposed against the adapting field. Six rats for each group were used for the ERG analysis. A: For the light-adapted condition, cone responses were not recorded for mutant-type rats at all intensities while at higher intensities cone responses were detected for wild-type rats clearly. B: Cone responses were clearly stimulated by 0.3 cd s $m^{-2}$ flashes in wild-type rats. The amplitudes for $X^{+}Y$ genotype rats were higher than for $X^{mcd}X^{+}$ rats and there was a significant difference for standard flashes ($^{**}p < 0.01$).

### 3.2. Histological analysis

To determine whether changes in the retinal structure were responsible for the abnormal ERGs, stained sections and whole retinas from mutant rats of ages between 1 and 12 months were compared with their respective control rats. For this age range, no abnormalities could be seen in the mutant rat retinas as illustrated in Fig. 3. In no case was there a significant difference between a control and mutant rat as shown in Fig. 4.

### 3.3. mcd locus mapping to the telomeric region of chromosome X

The *mcd* locus showed a linkage relationship with *DXRat21* and *DXRat96*, and was mapped to the telomeric region of chromosome X. Haplotype analysis revealed that the gene orders and genetic distances in centiMorgans (cM) were as follows: *DXRat96*:16.2 cM, *DXRat21*:12.2 cM, *mcd*, telomere, see Fig. 5A. The *mcd* locus spanned the 27.8-Mb region from point 132.9 to point 160.7 Mb on chromosome X (RGSC_v3.4).

### 3.4. mcd locus identification as a mutant splice acceptor site allele of the rat Opn1mw gene

The *mcd* locus was mapped to the telomeric region of chromosome X. Within this region, 169 genes have previously been mapped. *Opn1mw* was the strongest candidate gene among them since mutations in this gene are responsible for colorblindness in humans (Bonilha et al., 2005; Downes et al., 2001; Jiang et al., 2005). Sequencing analysis of *Opn1mw* gene exons revealed the presence of a G-to-T substitution in the invariant AG dinucleotide at the splicing acceptor site of intron 4 of the MCD rat as shown in Fig. 5B. The mutation was entirely associated with the mutant phenotypes of 441 progeny rats. Furthermore, the substitution was specific to the MCD rat among 156 inbred strains that we previously examined for which data is not shown. These findings suggested

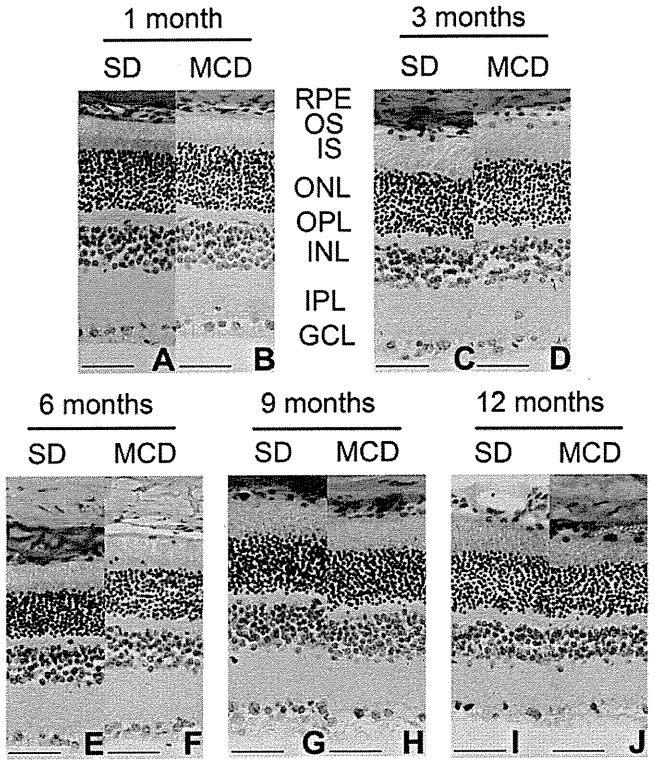


**Fig. 3.** Representative histological sections of SD and MCD rat retinas at 1, 3, 6, 9 and 12 months. A, C, E, G, and I, SD rat retina; B, D, F, H, and J, MCD rat retina. No morphologic abnormalities were apparent in the affected rats. RPE, retinal pigment epithelium; OS, outer segment, IS, inner segment; ONL, outer nuclear layer; OPL, outer plexiform layer; INL, inner nuclear layer; IPL, inner plexiform layer; GCL, ganglion cell layer. The bar denotes 50 μm in length.

that the G-to-T substitution of *Opn1mw* is likely to be responsible for the *mcd* mutant phenotype.

### 3.5. *Opn1mw transcript and M-opsin protein expression in the MCD retina*

To examine whether the point mutation in the *Opn1mw* gene could influence the Opn1mw transcript expression level, we performed quantitative real-time PCR analysis. Opn1mw transcripts were found to be nearly absent in the MCD retina as detailed in Fig. 6A. The Opn1mw transcript level in the MCD rat, normalized against that of GAPDH, was significantly lower than that in control rats at $5.1 \pm 2.9 \times 10^{-6}$ vs. $4.2 \pm 1.6 \times 10^{-2}$ ($p < 0.005$). These findings suggested that the G-to-T splice site substitution might have led to significant down-regulation of Opn1mw expression in MCD rats.

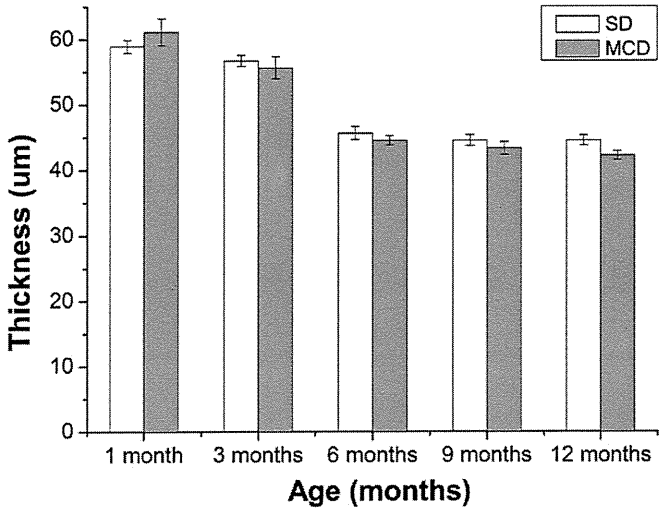


**Fig. 4.** Mean outer nuclear thickness measurements of retinal layers for control and mutant rats. No significant difference was found between the control and mutant rats for the five age groups.

This was confirmed by immunohistochemical analysis with anti-M-opsin antibody that revealed significantly down-regulated expression of M-opsin in the cones of MCD rats as shown in Fig. 6B and C. It is therefore likely that the lack of M-opsin expression underlies the abnormal photopic ERG responses in these rats.

### 3.6. *Wholemount immunocytochemistry*

To determine whether mutation would infect the survival of cones, wholemount immunocytochemistry were counted. Cones were marked with PNA in both mutant and wild rats. M-opsin could only be expressed in SD rats (Fig. 7). Statistical results showed that there was no obvious difference in the average densities of cones at these five ages (Fig. 7K).

## 4. Discussion

Cone and cone-rod dystrophies which can cause color defects or colorblindness can be divided into stationary and progressive disorders according to the course of the disease (Kohl, 2009). Congenital color vision defects or colorblindness can also be classified as autosomal recessive (Chang et al., 2002; Michaelides et al., 2004a; Sidjanin et al., 2002), autosomal dominant (Bonilha et al., 2005; Downes et al., 2001; Jiang et al., 2005) and X-linked by the genetic mode of inheritance (Heckenlively and Weleber, 1986). Among Western Europeans, about 8% of males are color blind. The most frequently identified type is deuteranopia and the second most frequent type is protanopia. Males with deuteranopia or protanopia have abnormal cone function comprising middle- or long-light wavelength sensitivity respectively. The detrimental effects on being unable to discriminate between colors varies depending on the severity of the condition from birth and whether or not vision can be facilitated using unaffected cone and rod photoreceptors (Gardner et al., 2009; Michaelides et al., 2004b; Nathans et al., 1986). BCM is known as a rare X-linked disorder of color vision characterized by the absence of both red and green cone sensitivities. Blue cone monochromats have only rods and blue cones (Nathans et al., 1989). No naturally occurring mutant animal model is available that is similar to BCM disease. The MCD rat strain might therefore be a useful model for research.

Rods and cones exist in abundance in the human retina. They possess a macula lutea and fovea centralis and can easily differentiate colors and fine structures. In rats, most of the photoreceptor cells are composed of rods. In albino rats, cones make up only 0.85–1% of all photoreceptors (Deegan and Jacobs, 1993; Szél and Röhlich, 1992). Among them, about 7% are sensitive to blue light and the remainders are sensitive to green light (Szél and Röhlich, 1992; Jacobs et al., 2001).

In our research, stimuli of different intensities and frequencies were used to investigate the functions of cones in MCD rats. Results showed that amplitudes of wild-type rats recorded in scotopic and photopic conditions were higher than those recorded in mutant-type rats. And the amplitudes in heterozygous wild-type female rats were lower than wild-type male rats. The results showed that the mutation played a large role in the function of cones. However, the functionality of the rods appeared to be normal. The structures were normal compared with their control rats. Molecular analysis

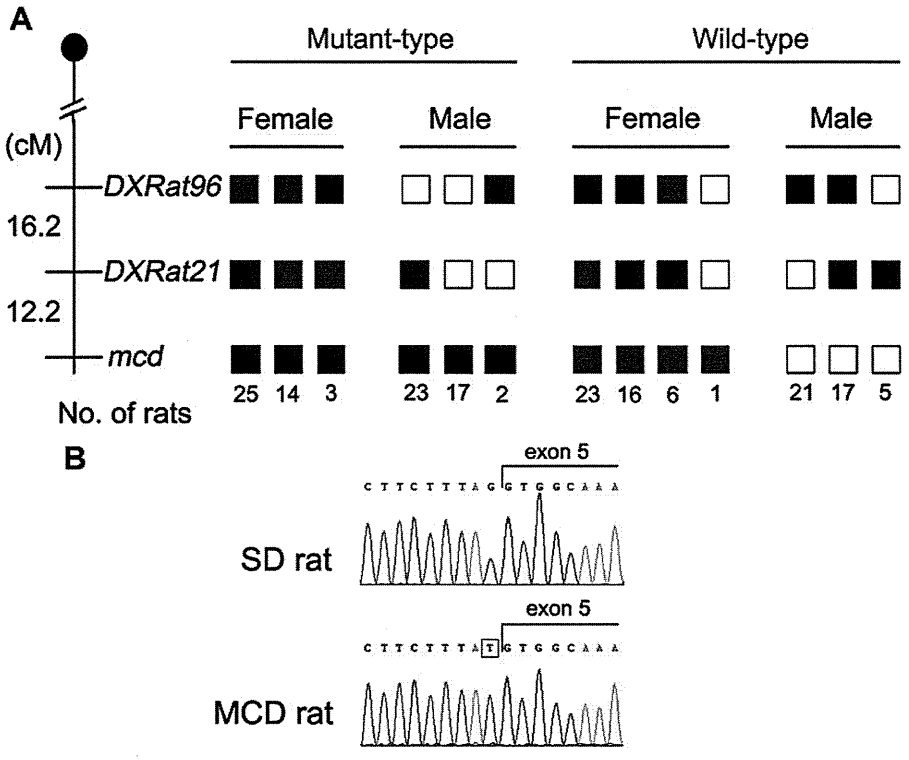


**Fig. 5.** Identification of the rat *mcd* mutation locus. A: Distribution of haplotypes observed among 173 progeny rats carrying a recombinant chromosome near *DXRat21* and *DXRat96*. Black boxes, homozygote for the *mcd* allele. White boxes, homozygote for the BN allele. Gray boxes, heterozygote for the *mcd* allele. B: Sequence analysis of *Opn1mw* DNA from homozygous SD ($X^{+}X^{+}$) and MCD ($X^{mcd}X^{mcd}$) rats. In the MCD ($X^{mcd}X^{mcd}$) rats, the nucleotide conversion G-to-T indicated by the box occurred at the invariant splicing acceptor site AG of intron 4.

showed that a point mutation in the *Opn1mw* gene caused down-regulation of its expression and that the translational level was responsible for ERG changes in the mutant rat. In humans, mutations in the *Opn1mw* gene cause deuteranopia. However, a detailed pathogenic pathway for this has not been clearly elucidated.

Deuteranopia is common among Western European men. So far, the mutations that have been reported on are all rearrangements or point mutations in exons. BCM is a rare (prevalence of less than 1 in 100,000) X-linked ocular disorder, characterized by severely reduced color discrimination capacity, poor visual acuity, infantile

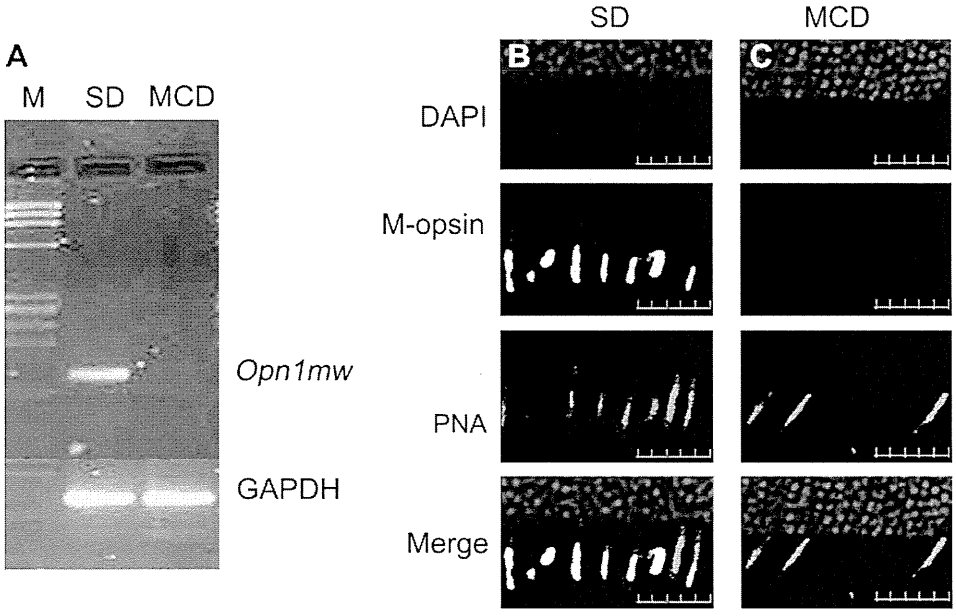


**Fig. 6.** Expression of *Opn1mw* transcripts and M-opsin protein in the retina of MCD rats. A: real-time PCR analysis of *Opn1mw* transcripts. *Opn1mw* expression was nearly absent in the retinas of the MCD rats. M; ϕX174/HaeIII digests. B, C: Immunohistochemical examination of M-opsin protein. B: Note that M-opsin was detected in the SD rats. C: M-opsin was not detected in the MCD rats. The bar denotes 50 μm in length.

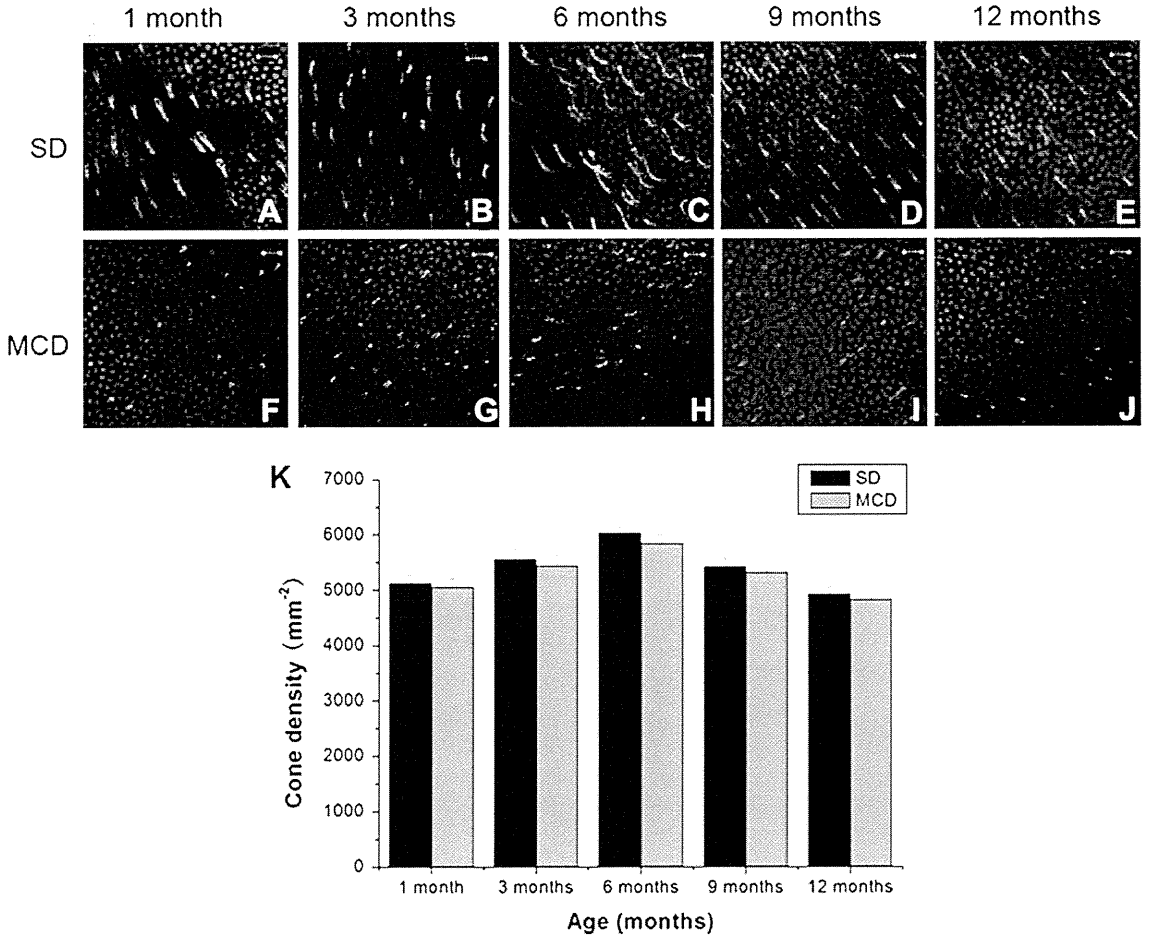


**Fig. 7.** Wholemount immunocytochemistry of the retinas from SD and MCD rats at 1, 3, 6, 9, 12 months. A, B, C, D, and E, SD rat retina; F, G, H, I, and J, MCD rat retina. Cones were marked with PNA in both SD and MCD rats. M-opsin could only be expressed in SD rats. K: Mean cone densities of SD and MCD rats. No significant difference was found between the control and mutant rats for the five age groups. The bar denotes 10 μm in length.

nystagmus and photophobia. The causes of BCM are mutations in the L and M pigment genes or in a region located near the L pigment gene that acts as a major regulatory region (called the locus control region, LCR) for expression of both the L and the M pigment genes. Deletions encompassing the LCR are a common cause of BCM (Deeb, 2004). Adult squirrel monkeys are missing the L-opsin gene. In this species, some females have trichromatic color vision whereas males are red–green color blind (Mancuso et al., 2009). Rats only have M- and S-opsin gene. The MCD rats are mutant with M-opsin gene and only have blue cones. We have reported here for the first time on a point mutation which results in a mutation that leads deuteranopia. The MCD rat model could be used to search for other upstream or downstream regulatory target genes that participate in forming the structure or as a model for BCM. In addition, characterizing mutant variants of the *Opn1mw* gene may provide important clues for structural and functional analyses of the corresponding protein. Identification of mutations similar to that which causes deuteranopia in humans has also permitted the elucidation of the molecular basis of this inherited disorder and furthered techniques for treatment and screening of the condition.

## Acknowledgements

The authors thank professors Rybaczki-Bullard of Ophthalmology and Molecular Genetics, University of Florida College of Medicine, Jijing Pang of Department of Ophthalmology, University of Florida College of Medicine, and Dr. Aaron B. Cowan for critical review of the manuscript. This study was supported by Grants 30571999 and 30872838 from the National Natural Science Foundation of China. It was also supported by Grants-in-aid for Cancer Research from the Ministry of Health, Labor and Welfare of Japan and Grants-in-aid for Scientific Research from the Japan Society for the Promotion of Science (21300153).

## References

Bonilha, V.L., Hollyfield, J.G., Grover, S., Fishman, G.A., 2005. Abnormal distribution of red/green cone opsins in a patient with an autosomal dominant cone dystrophy. Ophthalmic Genet. 26, 69–76.

Chang, B., Dacey, M.S., Hawes, N.L., Hitchcock, P.F., Milam, A.H., Atmaca-Sonmez, P., Nusinowitz, S., Heckenlively, J.R., 2006. Cone photoreceptor function loss-3, a novel mouse model of achromatopsia due to a mutation in Gnat2. Invest. Ophthalmol. Vis. Sci. 47, 5017–5021.

Chang, B., Hawes, N.L., Hurd, R.E., Davisson, M.T., Nusinowitz, S., Heckenlively, J.R., 2002. Retinal degeneration mutants in the mouse. Vis. Res. 42, 517–525.

Chang, B., Hawes, N.L., Hurd, R.E., Wang, J., Howell, D., Davisson, M.T., Roderick, T.H., Nusinowitz, S., Heckenlively, J.R., 2005. Mouse models of ocular diseases. Vis. Neurosci. 22, 587–593.

Deeb, S.S., 2004. Molecular genetics of colour vision deficiencies. Clin. Exp. Optom. 87, 224–229.

Deegan, J.F., Jacobs, G.H., 1993. On the identity of the cone types of the rat retina. Exp. Eye Res. 56, 375–377.

Downes, S.M., Holder, G.E., Fitzke, F.W., Payne, A.M., Warren, M.J., Bhattacharya, S.S., Bird, A.C., 2001. Autosomal dominant cone and cone-rod dystrophy with mutations in the guanylate cyclase activator 1A gene-encoding guanylate cyclase activating protein-1. Arch. Ophthalmol. 119, 96–105.

Gardner, J.C., Michaelides, M., Holder, G.E., Kanuga, N., Webb, T.R., Mollon, J.D., Moore, A.T., Hardcastle, A.J., 2009. Blue cone monochromacy: causative mutations and associated phenotypes. Mol. Vis. 15, 876–884.
Gu, Y.H., Zhang, Z.M., Long, T., Li, L., Hou, B.K., Guo, Q., 2003. A naturally occurring rat model of X-linked cone dysfunction. Invest. Ophthalmol. Vis. Sci. 44, 5321–5326.
Heckenlively, J.R., Weleber, R.G., 1986. X-linked recessive cone dystrophy with tapetal-like sheen. A newly recognized entity with Mizuo–Nakamura phenomenon. Arch. Ophthalmol. 104, 1322–1328.
Jacobs, G.H., Fenwick, J.A., Williams, G.A., 2001. Cone-based vision of rats for ultraviolet and visible lights. J. Exp. Biol. 204, 2439–2446.
Jiang, L., Katz, B.J., Yang, Z.L., Zhao, Y., Faulkner, N., Hu, J.B., Baird, J., Baehr, W., Creel, D.J., Zhang, K., 2005. Autosomal dominant cone dystrophy caused by a novel mutation in the GCAP1 gene (*GUCA1A*). Mol. Vis. 11, 143–151.
Kohl, S., 2009. Genetic causes of hereditary cone and cone-rod dystrophies. Ophthalmologe 106, 109–115.
Kuramoto, T., Kuwamura, M., Serikawa, T., 2004. Rat neurological mutations *cerebellar vermis defect* and *hobble* are caused by mutations in the netrin-1 receptor gene *Unc5h3*. Mol. Brain Res. 122, 103–108.
Mancuso, K., Hauswirth, W.W., Li, Q., Connor, T.B., Kuchenbecker, J.A., Mauck, M.C., Neitz, J., Neitz, M., 2009. Gene therapy for red–green colour blindness in adult primates. Nature 461, 784–788.
Michaelides, M., Aligianis, I.A., Ainsworth, J.R., Good, P., Mollon, J.D., Maher, E.R., Moore, A.T., Hunt, D.M., 2004a. Progressive cone dystrophy associated with mutation in CNGB3. Invest. Ophthalmol. Vis. Sci. 45, 1975–1982.
Michaelides, M., Hunt, D.M., Moore, A.T., 2004b. The cone dysfunction syndromes. Br. J. Ophthalmol. 88, 291–297.
Nakanishi, S., Kuramoto, T., Serikawa, T., 2009. Simple genotyping method using Ampdirect® plus and FTA® technologies: application to the identification of transgenic animals and their routine genetic monitoring. Lab. Anim. Res. 25, 75–78.
Nathans, J., Davenport, C.M., Maumenee, I.H., Lewis, R.A., Hejtmancik, J.F., Litt, M., et al., 1989. Molecular genetics of human blue cone monochromacy. Science 245, 831–838.
Nathans, J., Hogness, D.S., 1984. Isolation and nucleotide sequence of the gene encoding human rhodopsin. Proc. Natl. Acad. Sci. U.S.A. 81, 4851–4855.
Nathans, J., Piantanida, T.P., Eddy, R.L., Shows, T.B., Hogness, D.S., 1986. Molecular genetics of inherited variation in human color vision. Science 232, 203–210.
Sidjanin, D.J., Lowe, J.K., McElwee, J.L., Milne, B.S., Phippen, T.M., Sargan, D.R., Aguirre, G.D., Acland, G.M., Ostrander, E.A., 2002. Canine *CNGB3* mutations establish cone degeneration as orthologous to the human achromatopsia locus *ACHM3*. Hum. Mol. Genet. 11, 1823–1833.
Szél, A., Röhlich, P., 1992. Two cone types of rat retina detected by anti-visual pigment antibodies. Exp. Eye Res. 55, 47–52.
Ueyama, H., Kuwayama, S., Imai, H., Tanabe, S., Oda, S., Nishida, Y., Wada, A., Shichida, Y., Yamade, S., 2002. Novel missense mutations in red/green opsin genes in congenital color-vision deficiencies. Biochem. Biophys. Res. Commun. 294, 205–209.
Winderickx, J., Battisti, L., Motulsky, A.G., Deeb, S.S., 1992a. Selective expression of human X chromosome-linked green opsin genes. Proc. Natl. Acad. Sci. U.S.A. 89, 9710–9714.
Winderickx, J., Sanocki, E., Lindsey, D.T., Teller, D.Y., Motulsky, A.G., Deeb, S.S., 1992b. Defective color vision associated with a missense mutation in the human green visual pigment gene. Nat. Genet. 1, 251–256.
Xie, B., Guo, Q., An, J., Xia, F., Song, M.X., Li, L., Zhang, Z.M., 2008. Basic physiological and biochemical data in rats with retinal cone degeneration. Chin. J. Comp. Med. 4, 56–60.
Yanagi, Y., Takezawa, S., Kato, S., 2002. Distinct functions of photoreceptor cell-specific nuclear receptor, thyroid hormone receptor β2 and CRX in cone photoreceptor development. Invest. Ophthalmol. Vis. Sci. 43, 3489–3494.
Zhang, Z.M., Gu, Y.H., Guo, Q., Long, T., Li, L., Shi, L., Hou, B.K., 2004. Guideline for visual electrophysiological testing experiment in mice and rat. Rec. Adv. Ophthalmol. 2, 81–83.
Zhang, Z.M., Gu, Y.H., Long, T., Li, L., Guo, Q., 2002. Visual electrophysiological properties of a retinal cone cell degeneration rat. J. Fourth Mil. Med. Univ. 23, 986–989.

BRAIN RESEARCH 1328 (2010) 171–180

available at www.sciencedirect.com

ScienceDirect

www.elsevier.com/locate/brainres

BRAIN RESEARCH

Research Report

# Hippocampal cell loss and propagation of abnormal discharges accompanied with the expression of tonic convulsion in the spontaneously epileptic rat

*Ryosuke Hanaya*[a,*], *Masashi Sasa*[b], *Sei Sugata*[a], *Mai Tokudome*[a], *Tadao Serikawa*[c], *Kaoru Kurisu*[d], *Kazunori Arita*[a]

[a]*Departments of Neurosurgery, Graduate School of Medical and Dental Sciences, Kagoshima University, Kagoshima 890-8544, Japan*
[b]*Nagisa Clinic, Hirakata 573-1183, Japan*
[c]*Institute of Laboratory Animals, Graduate School of Medicine, Kyoto University, Kyoto 606-8501, Japan*
[d]*Department of Neurosurgery, Graduate School of Biomedical Sciences, Hiroshima University, Hiroshima, 734-8551, Japan*

ARTICLE INFO

*Article history:*
Accepted 28 February 2010
Available online 6 March 2010

*Keywords:*
Spontaneous epileptic rat (SER)
Hippocampal cell loss
Sprouting of mossy fiber
Brain-derived neurotrophic factor (BDNF)
Hippocampal sclerosis

ABSTRACT

Spontaneously epileptic rats (SER) are double mutants with both tonic convulsion and absence-like seizures from the age of 8 weeks. Hippocampal CA3 neurons in SER display a long-lasting depolarizing shift accompanied by repetitive firing (attributed to abnormalities of the $Ca^{2+}$ channels) with a single stimulation of the mossy fibers. In the present investigation, we examined if the seizure discharges of SER were correlated with the hippocampal abnormality of SER using electrophysiological and histological methods. In CA1 neurons of seizure-susceptible mature SER, higher-voltage (<8–11 V) stimulations induced a long depolarization shift (in 25% of neurons) with repetitive firing (in 12.5% of neurons). However, the tremor rat, one of the parent strains of SER, did not exhibit such abnormal firing in the CA3 region of the hippocampus. The number of CA3 neurons in SER was significantly ($p<0.01$) lower than that in tremor rats and Wistar rats, although no significant difference was established in the hilus. Sprouting of mossy fiber was observed in the dentate of mature SER; however, negligible staining was spotted in the dentate of both mature tremor and Wistar rats. Interestingly, expression of the brain-derived neurotrophic factor was higher in the hilus, CA3, and granular cell layer of dentate gyrus in SER than normal Wistar rats. The expression levels of TUNEL, bax, and Caspase-3 did not show significant changes between the SER and Wistar rats. SER exhibited hippocampal sclerosis-like changes which did not have enough potential for epileptogenesis. Repetitive tonic seizures and vulnerable CA3 neurons of SER could be involved in the induction of sclerosis-like changes in the hippocampus.



## 1. Introduction

Spontaneously epileptic rats (SER; *zi/zi*, *tm/tm*) are double mutants derived by mating heterozygote tremor rat (*tm/+*), a mutant found in the inbred colony of Kyoto–Wistar rats (Yamada et al., 1985), with a homozygote zitter rat (*zi/zi*) found in a Sprague–Dawley colony (Rhem et al., 1982). After 8 weeks of age, SER spontaneously show tonic convulsions

* *Corresponding author.* Department of Neurosurgery, Graduate School of Medical and Dental Sciences, Kagoshima University, 8-35-1 Sakuragaoka, Kagoshima 890-8544, Japan. Fax: +81 99 265 4041.
E-mail address: hanaya@m2.kufm.kagoshima-u.ac.jp (R. Hanaya).

0006-8993/$ – see front matter © 2010 Elsevier B.V. All rights reserved.
doi:10.1016/j.brainres.2010.02.086

and absence-like seizures characterized by sudden immobility and empty-staring. Cortical and hippocampal electroencephalograms (EEG) portray tonic convulsions and absence-like seizures accompanied by low-voltage fast waves and 5–7 Hz spike-wave-like complexes, respectively (Serikawa and Yamada, 1986; Sasa et al., 1988). In fact, the profile of antiepileptic drugs in SER has been demonstrated to be analogous to that of human absence seizures and tonic convulsions (Sasa et al., 1988). We have indicated that hippocampal CA3 pyramidal neurons in SER show a long-lasting depolarizing shift accompanied by repetitive firing when the mossy fibers (MF) are mimicked with a single stimulation (Ishihara et al., 1993); this abnormal excitability is attributable to abnormalities of the $Ca^{2+}$ channels (Yan et al., 2007). $Ca^{2+}$ influx in CA3 neurons is enhanced when MF was mimicked with a single stimulation (Amano et al., 2001), and this excessive $Ca^{2+}$ condition most likely impairs excitability of CA3 neurons (Limbrick et al., 2003).

Hippocampal abnormality is often related to temporal lobe epilepsy. Status epilepticus elicited by various methods induces brain lesions (including the hippocampus), and lesion-related reconstruction of the neuronal network in the hippocampus in turn triggers recurrent seizures, to induce temporal lobe epilepsy (Sloviter, 2008). Aberrant sprouting and synaptic reorganization of the MF axons are commonly found in the hippocampus of patients with temporal lobe epilepsy, resulting in structuring excitatory feedback loops in the dentate gyrus (Koyama et al., 2004). Brain atrophy (including the hippocampus) is often accompanied with recurrent generalized tonic–clonic convulsions. However, the focus-related findings of the hippocampus did not coincide with those of the genetic epilepsy model, where generalized tonic or tonic–clonic seizures are commonly observed.

It is well known that the cerebral cortex and thalamus interact to form spike-wave complexes (Danober et al., 1998; Luhmann et al., 1995). In some genetic epilepsy models, the hippocampus displays certain abnormal characteristics (Qiao and Noebels, 1993; Sirvanci et al., 2003), and atypical findings in the limbic system may be attributable to the development of absence seizures (Tolmacheva et al., 2004). From these reports, each seizure in SER could influence and probably potentiate neuronal activities of the hippocampus. CA3 discharges propagating to CA1 via the trisynaptic pathway involve activation of the Schaffer collaterals (Avoli et al., 2002). However, another report suggests that petit mal seizures do not propagate to the hippocampus and are not causally related to sprouting of the MF fibers (Kandel et al, 1996). The brain-derived neurotrophic factor (BDNF) in particular has important roles in regulating neural development and cell survival, as well as essential to molecular mechanisms of synaptic plasticity and larger scale structural rearrangements of axons and dendrites (Binder, 2007). The effects of BDNF in area CA3 are similar to those produced by bath application of low doses of kainic acid, which is thought to modulate glutamate release from MF terminals by a presynaptic action (Scharfman, 1997). The CA3 neurons of SER are hypersensitive to glutamate (Hanaya et al., 1998), and BDNF effects might to be modulated in the hippocampus of SER.

The tremor rat, which is one of the parent strains of SER, displays absence-like seizures (Yamada et al., 1985; Serikawa et al., 1987). The profile of antiepileptic drugs in tremor rats is analogous to that of absence seizures in humans and SER (Hanaya et al., 1995). Aspartoacylase-encoded genomic deletion is founded in tremor rats (Kitada et al, 2000), and aspartoacylase and atractin double-mutant mice exhibit both absence-like seizures and tonic convulsions, as observed in SER (Gohma et al., 2007). A comparative study of these two strains is most likely to clarify the relationships between the seizures and hippocampus. We examined hippocampal slices electrophysiologically and histologically to confirm the hippocampal abnormality observed in SER.

## 2. Results

### 2.1. *Intracellular recording*

The data were obtained from hippocampal neurons with a resting membrane potential of >−45 mV. In SER, abnormal firing was elicited in 7 of 10 CA3 neurons (Fig. 1) with the stimulation under 8 V; a ratio which has repeatedly been demonstrated in our previous study (Ishihara et al, 1993). In

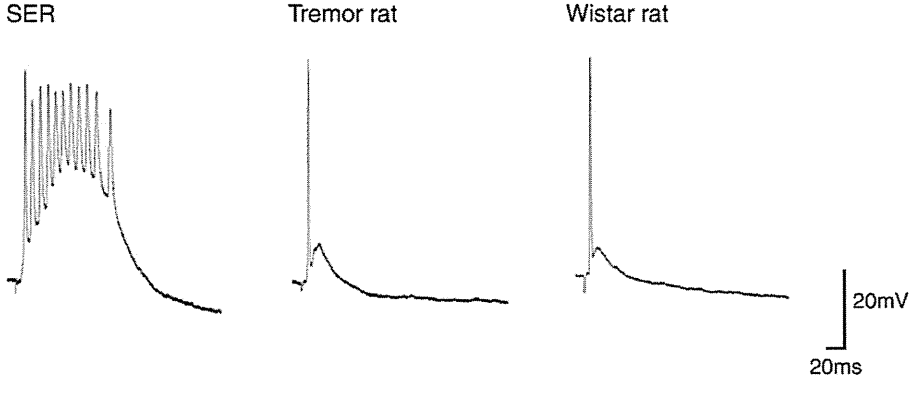


**Fig. 1 – Action potentials in hippocampal CA3 neurons induced by mossy fiber (MF) stimulation in spontaneously epileptic rats (SER), tremor and normal Wistar rats. The depolarization shift accompanied with repetitive firing was induced by a single stimulation in SER with seizures. Only a single action potential was induced by a single stimulation in mature tremor rats with seizures and normal age-matched Wistar rats.**

CA1 neurons of mature SER, stimulations with a higher voltage (>8–11 V) induced long depolarization shift (4/16 neurons) and repetitive firing (2/16 neurons) (Fig. 1). The mean duration of depolarization shift elicited in CA1 was longer than that in CA3. In contrast, such depolarization shift and repetitive firing were not observed in any of the five CA1 and six CA3 neurons in the hippocampus of mature Wistar rats, and only one action potential was obtained with MF stimulations (Fig. 2). Abnormal firing was not induced in either CA1 or CA3 neurons of immature SER and Wistar rats by stimulations of the MF or Schaffer collateral. Furthermore, MF stimulations did not induce abnormal responses in any of the nine CA3 neurons in the hippocampus of tremor rats (Fig. 1). The input impedance was lower in neurons with abnormal firing than in those without firing. All profile details of intracellular recording are described in Table 1.

### 2.2. *Histological study*

#### 2.2.1. *Hippocampal neurons*

During the immature period, the number of hippocampal neurons was evenly distributed in each area. In mature rats, the number of CA3 neurons registered 26.75±1.62 in SER; a count which was significantly ($p<0.01$) lower than those found in tremor rats (30.50±1.16 neurons) and in Wistar rats (33.25± 2.71 neurons). The CA3 cell counts of 11- to 12-week-old SER decreased significantly ($p<0.01$) more than that of Wistar rat. Although the number of CA3 neurons in 11- to 12-week-old SER did not show significant decreases, the CA3 neuronal count of SER showed a decreasing tendency with age. The neuronal counts in the other regions did not show significant differences between any two of the three mature strains (Figs. 3 and 4, Table 2).

### 2.3. *Sprouting of MF in the dentate gyrus*

Sprouting of MF was observed in the inner molecular layer of the dentate gyrus in mature SER of 13 to 15 weeks of age (Fig. 5). MF sprouting was negligible and non-existent in the strata oriens of CA3 and CA1, respectively. In fully mature tremor and Wistar rats (age: 48–66 weeks), meager deposition of zinc-positive granules in the granular layer of the dentate gyrus was observed. The extent of sprouting was ranked according to the sprouting score (Cavazos et al., 1994). Sprouting scored higher in SER than aged tremor and Wistar rats (Table 3).

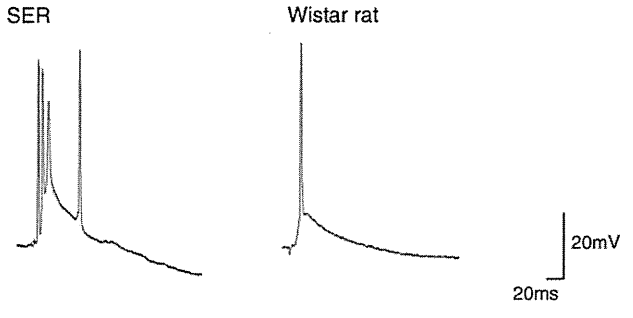


**Fig. 2 – Action potentials in CA1 neurons induced by Shaffer collateral stimulations of tremor rats with absence-like seizures. The depolarization shift accompanied with repetitive firing was induced by a single stimulation in spontaneously epileptic rats (SER) with seizures. Only a single action potential was induced by a single stimulation in normal age-matched Wistar rats.**

#### 2.3.1. *Immunohistochemical findings*

Analysis of BDNF immunoreactivity, expressed as the optical density, was performed after correction for background density. The densitometry levels of BDNF immunoreactivity were higher in the hilus, pyramidal layer and Stria orience of CA3, and dentate gyrus in SER than those found in normal Wistar rats (Table 4). SER did not indicate TUNEL-positive neurons at the fully mature stage. Caspase-3 is one of the key executioners of apoptosis, and Bax is one proapoptotic protein of the Bcl-2 family. Neither caspase-3 nor bax immunoreactive neurons were found in SER (Fig. 6).

## 3. Discussion

Hippocampal sclerosis is histologically characterized by neuronal loss and glial proliferation, especially at sites mainly located in the hilus of the dentate gyrus and in the CA1 and CA3 pyramidal cell layers (Bote et al., 2008). It is well known that hippocampal abnormalities and interactions with the limbic network contribute to mesial temporal lobe epilepsy in experimental epilepsy models. Patients with typical mesial temporal lobe epilepsy usually have medical histories often characterized with an initial precipitating injury, and they are likely to have hippocampal sclerosis in their surgical specimens (Mathern et al., 1996). In the dentate gyrus, morphological alterations induced by kindled seizures include the loss of polymorphic neurons in the hilus, axonal sprouting of MF, and synaptic reorganization of the MF pathway (Cavazos et al., 1994). In the hippocampus, prolonged hyperactivity induces MF sprouting with subsequent network reorganization, and BDNF is necessary to evoke this pathogenic plasticity. Basic activity-related changes in the central nervous system (CNS) are thought to depend on BDNF modulation of synaptic transmission (Binder, 2007). In the SER hippocampus exhibiting epileptic seizures, granule cells and pyramidal neurons express BDNF messenger RNA and BDNF-like immunoreactivity (Schmidt-Kastner et al., 1996), and the BDNF/trkB neurotrophin system may play a central role in the development of seizures in an animal model for temporal lobe epilepsy (Hughes et al., 1999). BDNF increased responses to a single afferent stimulus in selective pathways in the majority of slices. In area CA3, responses to MF stimulation increased in 73% of slices. These areas also demonstrated hyperexcitability after repetitive stimulations (Scharfman et al., 1998). This finding indicated that a single MF stimulation induced repetitive firing with a long depolarization shift due to chronically increased BDNF in the hippocampus. Hyperexcitation induces upregulation of BDNF protein expression in the MF pathway; an effect mediated by the L-type $Ca^{2+}$ channels (Koyama et al., 2004).

Tremor rats, a model for absence seizures (Serikawa et al., 1987), did not display hippocampal neuronal loss. In the dentate gyrus, tremor rats exhibited limited sprouting which

**Table 1 – Profiles of intracellular recording in SER, tremor and normal Wistar rats.**

| | SER | | | Tremor | Wistar | |
|---|---|---|---|---|---|---|
| | Immature | Mature without abnormal firing | Mature with abnormal firing | Mature | Immature | Mature |
| CA1 | $n=8$ | $n=12$ | $n=4$ | | $n=5$ | $n=5$ |
| Input impedance (MΩ) | 28.68±3.34 | 26.86±4.48 | 20.93±3.88*,*** | | 27.08±4.81 | 25.24±3.95 |
| Membrane potential (mV) | 58.99±9.07 | 57.58±5.94 | 57.18±10.13 | | 55.32±3.73 | 55.88±3.92 |
| Number of spikes | 1.00±0.00 | 1.00±0.00 | 4.00±0.00 ($n=2$) | | 1.00±0.00 | 1.00±0.00 |
| Deporalization shift (ms) | | | 104.18±11.35 | | | |
| CA3 | $n=5$ | $n=3$ | $n=7$ | $n=9$ | $n=6$ | $n=6$ |
| Input impedance (MΩ) | 29.54±1.58 | 32.53±2.31 | 19.05±0.65*,*** | 29.59±5.97 | 29.25±2.85 | 28.58±4.04 |
| Membrane potential (mV) | 57.00±5.70 | 58.67±4.04 | 58.21±7.23 | 55.13±5.79 | 57.00±7.07 | 53.35±5.91 |
| Number of spikes | 1.00±0.00 | 1.00±0.00 | 4.14±1.68**,*** | 1.00±0.00 | 1.00±0.00 | 1.00±0.00 |
| Deporalization shift (ms) | | | 72.57±18.15 | | | |

* $P<0.01$ significantly different from immature and mature Wistar rats.
** $P<0.01$ significantly different from immature SER and mature SER without abnormal firing.
*** $P<0.01$ significantly different from tremor rats.

was not significantly different from that of Wistar rats. This finding suggests that the inherited background of absence epilepsy does not enhance the incidence of hippocampal sclerosis. Genetic absence epilepsy rats (GAERS), one of the animal models for absence epilepsy, do not show any sprouting in the hippocampus (Sirvanci et al., 2003). When status epilepticus is induced in GAERS, nonepileptic control rats, and Wistar rats, the latency of spontaneous motor seizures in Wistar rats is shorter than those of GAERS and nonepileptic rats (Hanaya et al., 2008). Intraamygdaloid injection of kainic acid has revealed lower mossy fiber sprouting in GAERS than in Wistar rats (Gurbanova et al., 2008). These findings indicate that the Wistar rat, a parent strain of the tremor rat, appears to have a naïve hippocampus for accommodating stress; a feature which should also be inherited by the tremor rat. Neuronal changes in the SER

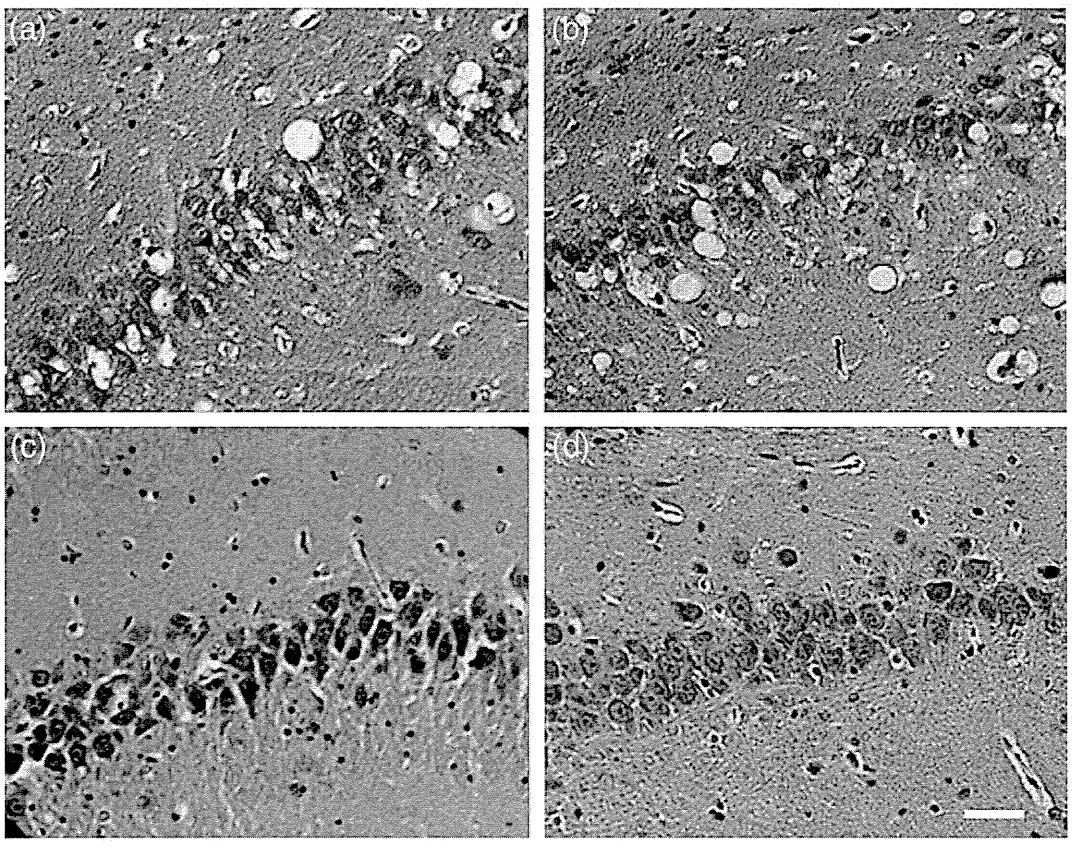


**Fig. 3 – The CA3 pyramidal cell layers of the immature spontaneously epileptic rats (SER) (a), mature SER (b), tremor rats (c), and Wistar rat (d). The CA3 pyramidal layer of mature SER was thin and neuronal count was lower than those of immature SER and the other two strains. Quantification of these differences can be found in Table 3. The scale bar represents 50 μm.**

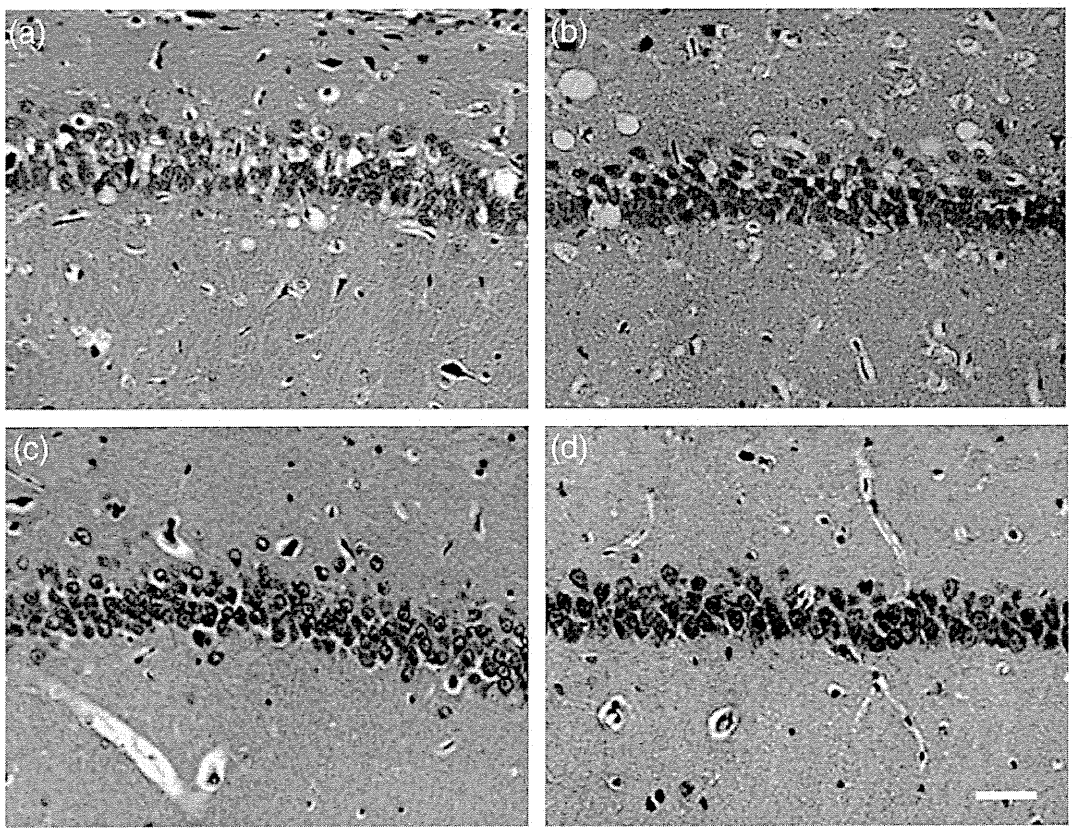


**Fig. 4 – The CA1 layer of the immature spontaneously epileptic rats (SER) (a), mature SER (b), tremor rats (c), and Wistar rat (d). The scale bar represents 50 μm. Neuronal counts did not show significant differences in each of the four groups of animals.**

hippocampus have partially revealed findings of hippocampal sclerosis. Interictal local cerebral glucose utilization in 13-week-old SER with epileptic seizures is generally lower than in the other two strains (zitter and kyo–Wistar rats), particularly in the hippocampus and amygdale (Saji et al., 1993), thus suggesting that any epilepsy-related lesion in SER is most likely to be located in the hippocampus and amygdala.

For the expression of temporal lobe epilepsy, a latent seizure-free period after initial precipitating injury is necessary to reorganize the dentate and hippocampal neurons (Sloviter 2008). In pilocarpine-induced status epilepticus, animals with a greater degree of cell loss in the hippocampal CA3 field tend to show a delayed onset of chronic epilepsy, suggesting that the CA3 field represents one of the routes for seizure spread (Mello et al., 1993). When the status epilepticus is induced in the genetically epileptic rats, neuronal loss following status epilepticus is similar and particularly marked in the limbic forebrain and parahippocampal cortices without the

**Table 2 – Number of neurons in the hippocampus of SER, tremor and normal Wistar rats.**

| | SER | | | Tremor | Wistar | |
|---|---|---|---|---|---|---|
| | Immature ($n$=4) | 11–12 weeks ($n$=6) | 14–16 weeks ($n$=6) | Mature ($n$=4) | Immature ($n$=4) | Mature ($n$=6) |
| CA1 | | | | | | |
| Pyramidal layer | 49.14±2.03 | 49.22±1.83 | 49.98±2.16 | 53.75±2.71 | 49.53±4.85 | 51.86±0.83 |
| S. Orience | 2.06±0.48 | 2.06±0.49 | 2.37±0.51 | 2.19±0.26 | 1.83±0.82 | 2.33±0.42 |
| CA3 | | | | | | |
| Pyramidal layer | 30.56±2.58 | 25.81±1.10* | 21.15±1.26**,***,† | 30.19±1.13 | 30.25±2.08 | 33.25±3.03 |
| S. Orience | 1.75±0.50 | 1.77±0.29 | 1.42±0.27 | 1.63±0.21 | 1.71±0.50 | 1.70±0.30 |
| Hilus | 52.96±12.99 | 47.14±7.69 | 52.64±5.59 | 54.29±7.42 | 49.96±16.05 | 53.93±11.18 |
| S. radiatum | 7.42±2.83 | 7.42±1.17 | 8.08±1.49 | 5.13±1.41 | 6.00±1.19 | 6.80±0.56 |
| Dentate gyrus | 4.08±1.34 | 4.67±1.62 | 5.33±1.66 | 3.58±0.32 | 4.75±1.13 | 4.27±1.66 |

* $P<0.01$ significantly different from mature Wistar rats.
** $P<0.01$ significantly different from immature and mature Wistar rats.
*** $P<0.01$ significantly different from immature and aged 11–12 weeks SER.
† $P<0.01$ significantly different from tremor rats.

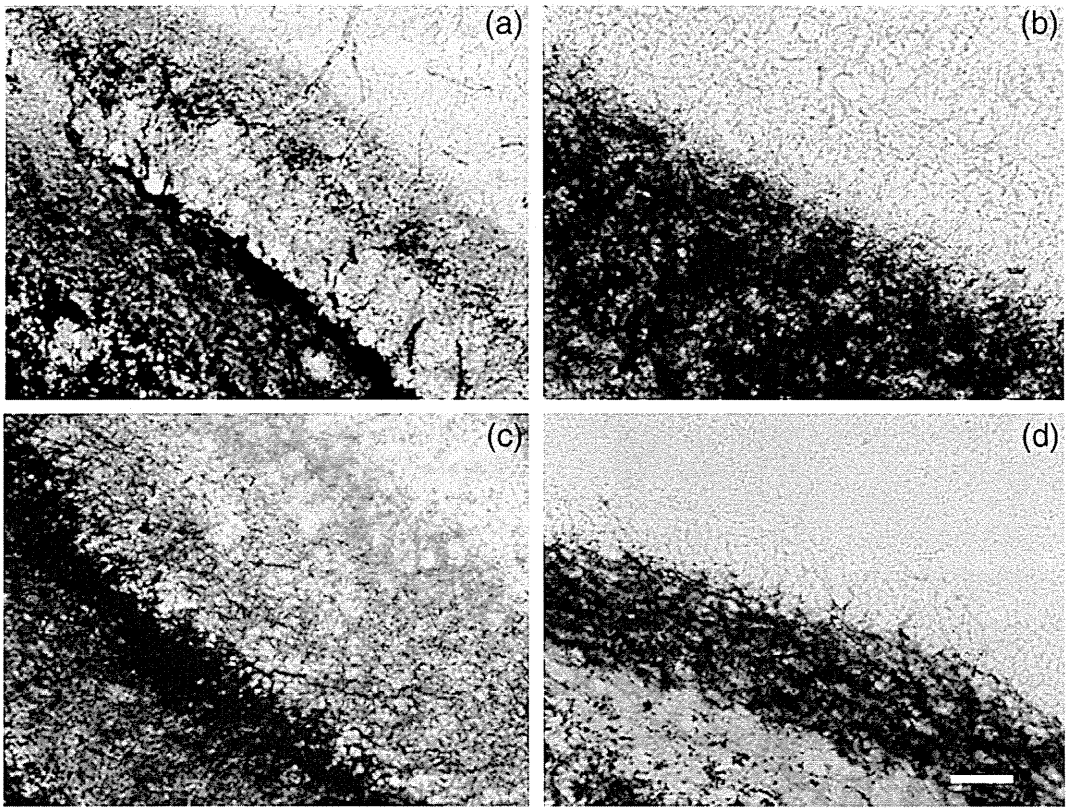


**Fig. 5 – Timm's staining of the dentate gyrus. Obvious sprouting was observed in mature spontaneously epileptic rats (SER) (a); however, no sprouting and negligible granules were observed in the mature tremor (b), fully mature tremor (c) rats, respectively. Granule deposits were not located in the Wistar rat (d). The scale bar represents 50 μm.**

semiology of seizures (Hanaya et al., 2008). In temporal epilepsy models induced by status epilepticus, the trisynaptic loop bypasses the classical trisynaptic hippocampal circuit without affecting the propagation of excitability (Scharfman 1997; Wozny et al., 2005), and CA1 hyperexcitability due to extensive CA3 pyramidal cell loss is attributable to a loss of excitatory inputs to area CA1 inhibitory basket cells (Sloviter, 1991).

In temporal lobes resected from drug-resistant epilepsy patients with mesial temporal lobe sclerosis, DNA fragmentation is not detected by TUNEL staining (Uysal et al., 2003; Xu et al., 2007). Positive immunostained neurons for bcl-2, and bax are found in the sclerotic hippocampi in both reports. Correlative analyses have revealed that the expression levels of p53, fas and caspase-3 are positively correlated with the seizure frequency (Xu et al., 2007). Neuronal death with fragmentation of DNA has also been observed in CA1 and CA3 regions of the status epilepticus-induced temporal lobe epilepsy model (Ebert et al., 2002; Weise et al., 2005). This cell death is, in fact, related to the initial status epilepticus rather than to the frequency of spontaneous seizures (Gorter et al., 2003). In SER, there were no TUNEL-positive neurons and bax- or caspase-3-immunoreactive neurons in the hippocampus of SER (as noted in the animal model of status epilepticus (Bengzon et al., 2002). Therefore, these findings indicate that CA3 neuronal loss in SER may not involve apoptosis.

**Table 3 – Sprouting scores of each strain.**

| | Mature ($n$=6) | Fully mature ($n$=6) |
|---|---|---|
| SER | 2.8±0.8* | |
| Tremor rats | 0.2±0.4 | 2.0±0.7** |
| Wistar rats | 0.4±0.5 | 1.2±0.4** |

* $P<0.01$ significantly different from other mature and fully mature strains.
** $P<0.01$ significant different from other mature and fully mature strains.

**Table 4 – BDNF expression in the hippocampus.**

| | SER ($n$=6) | Wistar ($n$=6) |
|---|---|---|
| CA1 | | |
| Pyramidal layer | 2.7±4.2 | −1.2±4.6 |
| S. Orience | 0.7±7.2 | −7.3±4.8 |
| CA3 | | |
| Pyramidal layer | 9.3±3.8** | −6.8±4.3 |
| S. Orience | −5.0±2.3** | −8.9±2.2 |
| Hilus | −0.2±4.7* | −7.0±4.1 |
| S. radiatum | 0.3±5.1* | −5.1±3.3 |
| Dentate gyrus | −0.7±5.6** | −13.4±4.2 |

* $P<0.05$.
** $P<0.01$ significantly different from Wistar rats.